

Wet-Stamped Precipitant Gradients Control the Growth of Protein Microcrystals in an Array of Nanoliter Wells

Goher Mahmud,[†] Kyle J. M. Bishop,[†] Yuriy Chegel,[†] Stoyan K. Smoukov,[†] and Bartosz A. Grzybowski^{*,†,‡}

Department of Chemical and Biological Engineering and Department of Chemistry, Northwestern University, 2145 Sheridan Road, Evanston, Illinois 60208

Received October 20, 2007; E-mail: grzybor@northwestern.edu

Protein crystals are important for the determination of 3D structures of proteins, binding affinities, and in pharmaceutical research.¹ Crystallization of proteins is often a laborious process requiring optimization of several experimental variables including, for example, temperature, pH, protein concentration, and the delivery rate of an appropriate precipitant.² In this context, there has recently been much interest in new experimental methods that would screen multiple crystallization conditions simultaneously, require minimal amounts of often-expensive reagents, and produce good quality crystals. Microfluidics³ has been widely used to achieve these objectives⁴ and several ingenious systems have been developed to produce X-ray quality microcrystals.^{5,6} Recently, Ismagilov's^{5,7} and Quake's⁸ groups have applied microfluidics to study the kinetics of crystal growth; these systems, however, have not yet produced quantitative information relating diffusive transport (e.g., rates of water evaporation or precipitant delivery) to crystal morphologies/sizes. Here, we describe a conceptually different experimental method that yields such information from a reaction-diffusion process⁹ initiated by wet stamping (WETS).¹⁰ In this approach, a hydrogel "stamp" is used to set up time-evolving, diffusive gradients of precipitant concentration over an array of gel-filled, nanoliter wells containing the protein (here, lysozyme). Because the precipitant flux varies with the distance from the stamp and with time, the array of wells realizes multiple growth conditions, which lead to crystals of various habits and dimensions. Importantly, statistical averaging over wells equidistant from the source of precipitant allows quantification of nucleation and growth rates that agree with those established in macroscale experiments. These results suggest that microscale RD can provide a basis for large-scale protein microcrystallization and for quantification of its key parameters.

Figure 1 illustrates the experimental arrangement (also see Supporting Information). First, nanoliter-volume wells ($100 \times 100 \times 100 \mu\text{m}^3$) in an oxidized PDMS master are filled with 1% w/v high-strength agarose (OminPur) and are soaked overnight in a 60 mg/mL protein solution (chicken egg white lysozyme, Sigma). A dialysis membrane (100 μm thick, D9777, Sigma-Aldrich) is then placed onto the surface, and a thin, 400 μm "transport layer" of 5% w/v agarose solution is applied. A 1 cm \times 1 cm \times 2 cm block ("stamp") of 10% w/v agarose soaked in 15% w/v of a precipitant (NaCl) is placed near the edge of the substrate, and the entire system is immersed under paraffin oil to minimize evaporation. The crystals are then grown for times $\tau_{\text{exp}} \approx 50$ h.

Unlike macroscopic setups for crystallization in gel media¹¹ where both the precipitant and the protein are free to diffuse, the dialysis membrane eliminates diffusion of protein out of the wells but allows diffusive delivery of the precipitant. In this way, each

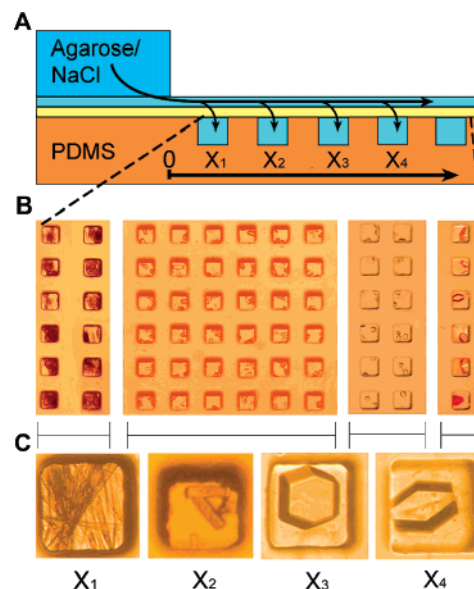


Figure 1. (a) Side view schematic of the experimental setup. Protein precipitant diffuses from the stamp through the transport layer (turquoise) and into the microwells (light blue) through a dialysis membrane (yellow). The entire assembly is immersed in paraffin oil. (b) An optical micrograph showing different regions of an array of wells containing lysozyme microcrystals. (c) Magnified images of typical crystals grown in the regions shown in panel b and corresponding to $x_1 \approx 4$ mm, $x_2 \approx 6$ mm, $x_3 \approx 16$ mm, $x_4 \approx 18$ mm. Side of each microwell = 100 μm . More images of the crystals are included in the Supporting Information.

well becomes a separate crystallization microreactor (Figure 1b), and the crystallization conditions are controlled by the rate of precipitant delivery. Specifically, the time-dependent concentration of the salt precipitate, C_s , at different locations, x , and times, t , can be approximated by solving (cf. Supporting Information) the one-dimensional diffusion equation $\partial C_s(x,t)/\partial t = D \partial^2 C_s(x,t)/\partial x^2$ over the $0 \leq x \leq L$ domain ($L \approx 2$ cm corresponds to the far-end of the substrate), with the diffusion coefficient of salt in 10% w/v agarose $D \approx 5 \times 10^{-6}$ cm²/s,¹⁰ and with the initial/boundary conditions $C_s(x,0) = 0$ (no salt in the wells at $t = 0$), $C_s(0,t) = C_s^0$ (delivery stamp maintains constant salt concentration), and $\partial C_s(L,t)/\partial x = 0$ (no diffusion through the far boundary at $x = L$).

Solution of the diffusion equation shows that the time-dependent concentrations profiles of precipitant are different for wells located at different distances, x , from the stamp (Figure 2a and Supporting Information). These differences, in turn, translate into different crystal growth conditions and affect the qualities and morphologies of the crystals that ultimately emerge (cf. Figure 1c). Close to the stamp ($x \approx 0$ –4 mm), where the flux is initially high, each well contains many ($N \approx 20$) small, needle-like crystals. Further away, where the delivery of precipitant is slower, the crystals become fewer, larger, and have plate-like, tetragonal morphologies typical

[†] Department of Chemical and Biological Engineering.

[‡] Department of Chemistry.

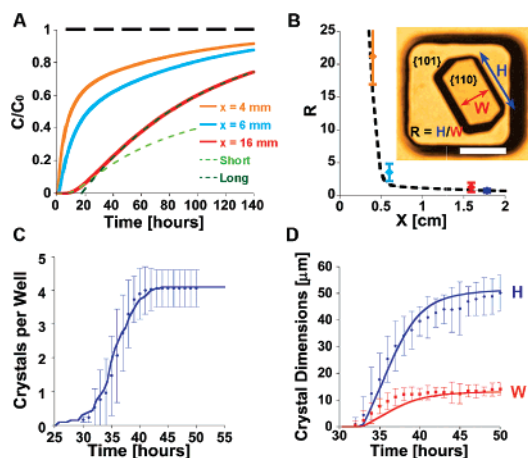


Figure 2. (a) Calculated time-dependencies of salt concentration, $C_S(x,t)$ in wells at different distances, x . Green dashed lines give examples of piecewise fits for short and long time scales (at $x = 16$ mm). Horizontal dashed line corresponds to $C_S = C_0$. (b) Dependence of the crystals' aspect ratios, R (defined in the inset), on x . Dashed line gives the fit obtained from the RD model of crystal nucleation/growth. Scale bar for the inset image = $50 \mu\text{m}$. (c) Numbers of crystals per well and (d) heights and widths for crystals grown in microwells at $x = 6$ mm. The lines are fits obtained from the RD model. In panels c and d, the average values and standard deviations are based on measurements of ca. 120 crystals from 6 independent array experiments per each data point.

of lysozyme. At $x > \sim 6$ mm, each well has, on average, $N = 4$ crystals and the zone over which crystals grow over the course of experiment extends to $x \approx 18$ mm. The aspect ratio, $R = H/W$, of the crystals decreases with increasing x (Figure 2b) and the crystals gradually change from having large {110} to large {101} faces.

It is important to emphasize that spatial variations in the sizes/dimensions of the crystals over the microwell array are not due to the ultimate concentrations of the precipitant (since in all wells, $C_S(x,t)$ asymptotically approaches the same value, C_0 ; Figure 2a) but rather due to different “schedules” of salt delivery. These schedules at a given location/well can be approximated piecewise by analytical functions: $C_S(x,t) \approx C_0 \operatorname{erfc}(x/\sqrt{4Dt})$ for short times (i.e., $tD/L^2 < 0.2$) and $C_S(x,t) \approx C_0[1 - (4/\pi) \sin(\pi x/2L) \exp(-\pi^2 Dt/4L^2)]$ for longer times. These dependencies might be useful in translating the results of microarray crystallization to other experimental settings, where to obtain crystals of morphologies similar to those observed in the microwells at location x , one should deliver the precipitant at a “diffusive-like” rate: $r_S = V\partial C_S(x,t)/\partial t$, where V is the volume of the crystallization vessel.

When the process of crystal growth is studied as a function of both x and time, t , the changes in the dimensions and numbers of microcrystals in the wells can be related—by reaction-diffusion modeling^{9,10}—to the underlying nucleation rates and the rates of growths of individual faces. In the RD model, the nucleation rate is expressed according to classical nucleation theory as $J = AC_P(x,t) \exp\{-B/[\ln(C_P(x,t)/C_P^*(x,t))]\}$, where A and B are constants¹² ($A = 60000$ crystals $\text{mg}^{-1} \text{min}^{-1}$; $B = 85$), $C_P(x,t)$ is the protein concentration, and $C_P^*(x,t) = (8.7 \times 10^{-4} \text{ w/v}) \exp[-C_S(x,t)/(1.8 \times 10^{-4} \text{ w/v})]$ determined previously² relates the solubility of lysozyme to the concentration of the salt (here, determined by the diffusion equation). In each time interval, Δt , a new crystal is nucleated in a well of volume V with probability, $p_{\text{nuc}} = JV\Delta t$. These equations are coupled to those describing the growth of each nucleated crystal i (of dimensions $\approx W_i \times H_i$ along the {110} and {101} faces, respectively) and to the equation describing protein depletion (for details, see Supporting Information):

$$\begin{aligned} dW_i/dt &= 2k_{110}C_P \ln(C_P/C_P^*)^{n_{110}}; \\ dH_i/dt &= 2.2k_{101}C_P \ln(C_P/C_P^*)^{n_{101}} \\ dC_P/dt &= -\sum_{i=1}^N (W_i^2 (dH_i/dt) + 2H_iW_i(dW_i/dt))/(v_P V) \end{aligned}$$

where $i = 1 \dots N$, the k 's are the growth rates of the crystal faces, n 's are constants for given growth conditions,¹³ and v_P is the molar volume of the protein crystal. For a given set of parameters, these coupled differential equations can be solved numerically and their solutions compared to experimentally measured quantities $N(t)$, $W(t)$, $H(t)$. Figure 2 parts c and d show one such comparison (here, for wells at $x = 6$ mm) where the experimental time-dependencies of the numbers of crystals per well and the dimensions of crystal faces agree with the values calculated by the RD equations. Figure 2b confirms that with the same simulation parameters A , B , k 's, and n 's, the model also reproduces experimental crystal dimensions for rows at other distances. Together these results suggest that the RD equations capture the key features of crystal-growth process and that, when applied to proteins other than lysozyme, they should be capable of extracting physically meaningful nucleation/growth parameters from the counts and morphologies of crystals grown in the array's microwells.

To summarize, we described a simple reaction-diffusion system in which spatiotemporal changes in the flux of precipitant control the growth of protein microcrystals over an array of microscopic wells. The major virtues of this system are that it realizes multiple crystal-growth conditions in a single experiment and can relate the qualities/dimensions of the forming microcrystals to the “schedule” of precipitant delivery and to the underlying nucleation/growth parameters. In the future, the reaction-diffusion approach could be extended to other precipitant/protein combinations and could provide a basis for a high-throughput platform with which to study and optimize protein crystallization.

Acknowledgment. This work was supported by the Pew Scholarship and NSF Career Award (to B.A.G.), Gates Fellowship (G.M.), and the NSF Fellowship (to K.J.M.B.)

Supporting Information Available: Experimental and modeling details and additional images of crystals. This material is available free of charge via the Internet at <http://pubs.acs.org>.

References

- (1) Durbin, S. D.; Feher, G. *Ann. Rev. Phys. Chem.* **1996**, *47*, 171.
- (2) (a) Rosenberger, F.; Howard, S. B.; Sowers, J. W.; Nyce, T. A. *J. Cryst. Growth* **1993**, *129*, 1. (b) Cacioppo, E.; Pusey, M. L. *J. Cryst. Growth* **1991**, *114*, 286. (c) Muschol, M.; Rosenberger, F. *J. Chem. Phys.* **1997**, *107*, 1953. (d) McPherson, A. *Eur. J. Biochem.* **1990**, *189*, 1. (e) Bhamidi, V.; Varanasi, S.; Schall, C. A. *Cryst. Growth Des.* **2002**, *2*, 5.
- (3) Squires, T. M.; Quake, S. R. *Rev. Mod. Phys.* **2005**, *77*, 977.
- (4) Zheng, B.; Gerds, C. J.; Ismagilov, R. F. *Curr. Opin. Struct. Biol.* **2005**, *15*, 548.
- (5) Song, H.; Chen, D. L.; Ismagilov, R. F. *Angew. Chem., Int. Ed.* **2006**, *45*, 7336.
- (6) Anderson, M. J.; Hansen, C. L.; Quake, S. R. *Proc. Nat. Acad. Sci. U.S.A.* **2006**, *103*, 16746.
- (7) Zheng, B.; Tice, J. D.; Roach, L. S.; Ismagilov, R. F. *Angew. Chem., Int. Ed.* **2004**, *43*, 2508.
- (8) Hansen, C. L.; Classen, S.; Berger, J. M.; Quake, S. R. *J. Am. Chem. Soc.* **2006**, *128*, 3142.
- (9) Grzybowski, B. A.; Bishop, K. J. M.; Campbell, C. J.; Fialkowski, M.; Smoukov, S. K. *Soft Matter* **2005**, *1*, 114.
- (10) (a) Campbell, C. J.; Smoukov, S. K.; Bishop, K. J. M.; Grzybowski, B. A. *Langmuir* **2005**, *21*, 2637. (b) Klajn, R.; Fialkowski, M.; Bensemam, I. T.; Bitner, A.; Campbell, C. J.; Bishop, K. J.; Smoukov, S.; Grzybowski, B. A. *Nat. Mater.* **2004**, *3*, 729.
- (11) Henisch, H. K. *Crystal Growth in Gels*; Dover: New York, 1996.
- (12) Bhamidi, V.; Varanasi, S.; Schall, C. A. *Cryst. Growth Des.* **2002**, *2*, 5.
- (13) Durbin, S. D.; Feher, G. *J. Cryst. Growth* **1986**, *76*, 3.

JA078051K